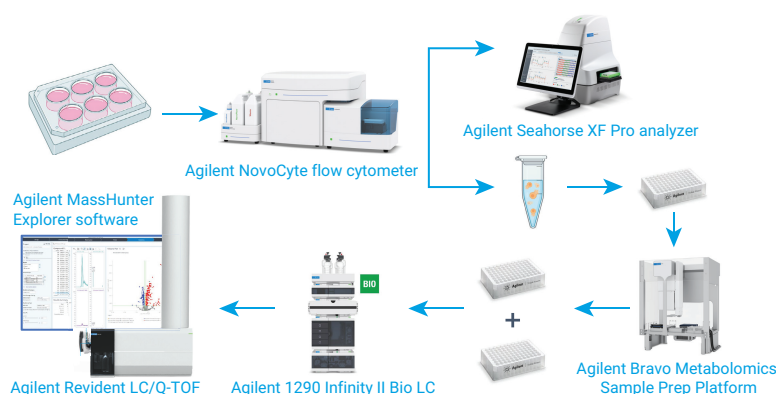


Illuminating the Cellular and Molecular Response to Drug Treatment by Combining Bioenergetic Measurements with LC/MS Omics



Authors

Mark Sartain,
Genevieve Van de Bittner,
Natalia Romero, James Pyke,
Yoonseok Kam,
Maria Apostolidi, and
Dustin Chang
Agilent Technologies, Inc.

Abstract

Combining multiple metabolic cell analysis techniques has the power to uncover new biological insights not revealed through any single analysis technique. In this application note, cellular-resolution Agilent Seahorse XF bioenergetic analyses were combined with molecular-resolution Agilent Revident Q-TOF LC/MS metabolomic and lipidomic analyses to investigate metabolic adaptations in drug-treated cancer cells. Tyrosine kinase inhibitor-treated leukemia cells exhibited reduced mitochondrial function and altered metabolic pathway use. It was only by combining mitochondrial function, metabolomic, and lipidomic insights that a new biological hypothesis was uncovered: the treated leukemia cells upregulated anaplerosis to overcome reduced mitochondrial function, but only in response to one of the two inhibitors. This multi-technique, cellular-to-molecular workflow can be used to uncover metabolic mechanisms of action and off-target effects of drug compounds.

Introduction

Cancer cells alter the production of building blocks and energetic metabolites through metabolic reprogramming.¹ Identifying the reprogrammed metabolic pathways within cancers and the metabolic pathway response to putative therapeutics is a promising strategy for developing novel therapeutic targets or combination therapies. To this end, complementary technologies can offer synergistic capabilities for deeper insight into drug-induced metabolic pathway modulation of cancer cells.

Specifically, analyses with the Agilent Seahorse XF Pro analyzer provide cellular resolution monitoring of metabolic flux through measurements of oxygen consumption rate (OCR) and extracellular acidification rate (ECAR). The rates of glycolysis and respiration observed through ECAR and OCR data provide a window into live cell function, since glycolytic and mitochondrial metabolic pathways play critical roles in a variety of cellular processes, including activation, proliferation, differentiation, cell death, and disease progression. Meanwhile, LC/MS-based omics and qualitative flux analyses provide molecular resolution monitoring of metabolic pathway modifications through measurements of metabolite abundances or their degree of isotope label incorporation.

This application note combines a wide portfolio of Agilent hardware, software, and assay kits in a comprehensive workflow (Figure 1) to study the metabolic pathway effects of two putative anticancer drugs from the tyrosine kinase inhibitor family. These two inhibitors were selected from a previous application note² where an 80-compound tyrosine kinase inhibitor library was screened with the Agilent Seahorse XF Real-Time ATP rate assay to assess acute effects of the inhibitors on glycolytic and mitochondrial ATP production rates.

To identify putative mechanisms of action for the metabolic impacts of the selected tyrosine kinase inhibitors, the Seahorse XF Real-Time ATP Rate Assay was repeated following a longer incubation period and the drug-treated cell characterization was extended by analyzing proton leak and spare respiratory capacity (SRC)—two measurements provided with the Agilent Seahorse XF Mito Stress Test. Independently, the selected tyrosine kinase inhibitors were assessed for their impact on molecular metabolism using metabolomic and lipidomic LC/MS analysis enabled by automated sample preparation with the Agilent Bravo Metabolomics Sample Prep Platform.³ Cell extracts were analyzed with the Agilent Revident LC/Q-TOF and MassHunter Explorer software in a discovery workflow, and LC/MS analyses were used to identify metabolic pathway perturbations.

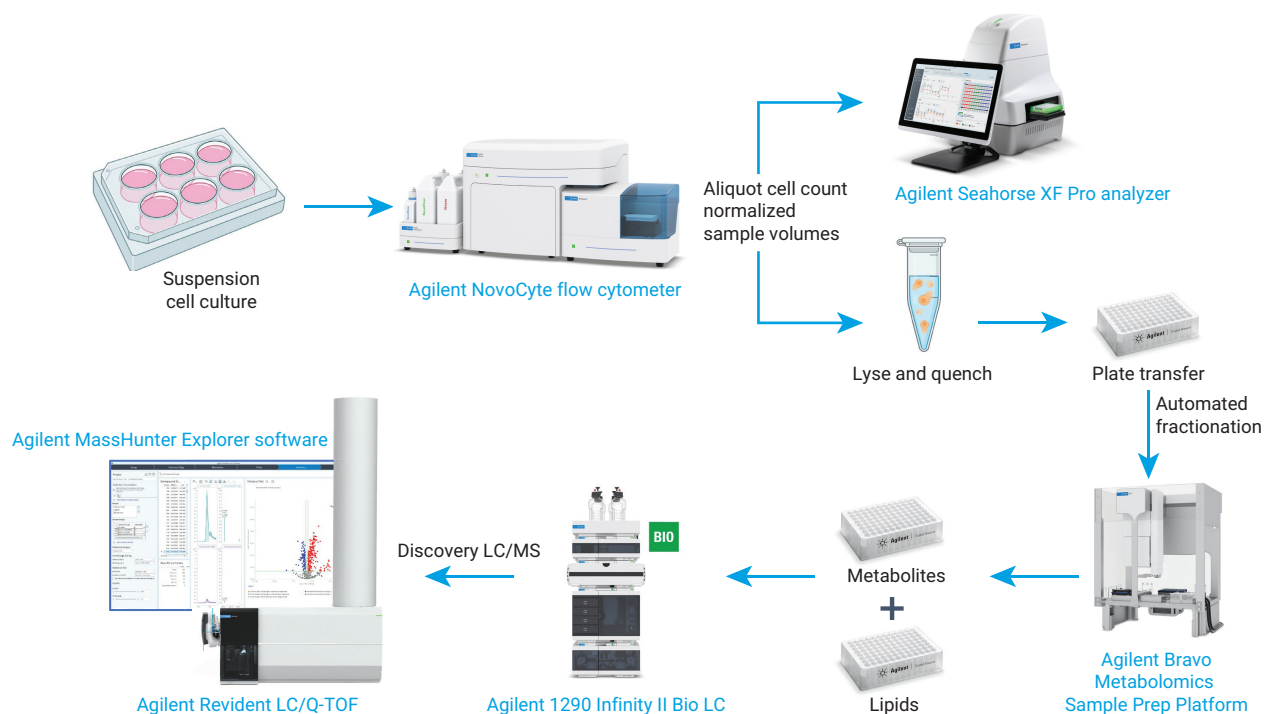


Figure 1. Overview of workflow, from cell culture to Seahorse XF, and from cell culture to automated sample preparation to Q-TOF LC/MS analysis. Key technologies highlighted in this application note are in blue. The cell culture plate and microtube portions of this image were created with BioRender.com.

Experimental

Materials

The THP-1 cell line was obtained from American Type Culture Collection and was cultured in complete Roswell Park Memorial Institute (RPMI) medium supplemented with 0.05 mM 2-mercaptoethanol (Life Technologies). Drug compounds AG-879 (99% HPLC grade) and SU1498 ($\geq 98\%$ HPLC grade), as well as the compound vehicle DMSO (sterile filtered), were purchased from MilliporeSigma.

Sample preparation solvents and chemicals

LC/MS-grade methanol (MeOH), NMR-grade trifluoroethanol (TFE), $\geq 99.5\%$ GC-grade dichloromethane, high-purity ($> 99.5\%$) ethanol, LC-grade or 99.9% pure butanol, and LC/MS-grade acetonitrile (ACN).

LC/MS mobile phase solvents and chemicals

Ammonium formate and ammonium acetate were purchased from Sigma-Aldrich (St. Louis, MO, U.S.). MeOH (hypergrade for LC/MS, LiChrosolv), ACN (hypergrade for LC/MS, LiChrosolv), and 2-propanol (hypergrade for LC/MS, LiChrosolv) were purchased from Supelco (Bellefonte, PA, U.S.). Ultrapure water for sample preparation and LC/MS analysis was produced with a Milli-Q Integral system equipped with a LC-Pak Polisher and a 0.22 μm point-of-use membrane filter cartridge (MilliporeSigma).

Instrumentation

The Agilent **NovoCyte Advanteon flow cytometer** (three lasers) coupled with the Agilent NovoSampler Q system (part number 2010201). Note that the Agilent NovoCyte Quanteon and Penteon flow cytometers are also suitable for this workflow when paired with a NovoSampler Q system. Data for this application note were collected using a NovoCyte Quanteon flow cytometer with NovoSampler Q system. The accessories and consumables used with the flow cytometer included:

- Agilent NovoCyte quality control and calibration particles (part number 8000004)
- Agilent NovoCyte large fluidic cart (part number 2010117AA)

The Agilent **Seahorse XF Pro analyzer** (product number S7855A) with the following consumables:

- Agilent Seahorse XF Real-Time ATP rate assay (part number 103592-100)
- Agilent Seahorse XF Cell Mito Stress Test kit (part number 103015-100)
- Agilent Seahorse XFe96/XF Pro PDL FluxPak Mini (part number 103798-100)

The Agilent **Bravo Metabolomics Sample Prep Platform** (product number G5589AA) with the following supplementary protocols:

- Supplementary Dual Metabolite + Lipid Cell Sample Preparation VWorks protocols (contact an Agilent automation workflow specialist for details)

The Agilent **1290 Infinity II Bio LC system** consisting of:

- Agilent 1290 Infinity II Bio high-speed pump (product number G7132A)
- Agilent 1290 Infinity II Bio multisampler with thermostat (product number G7137A)
- Agilent 1290 Infinity II multicolumn thermostat (product number G7116B) with an Agilent InfinityLab Quick Change 2-position/10-port Bio valve, 1,300 bar (product number G5641A)

The Agilent **Revident LC/Q-TOF** with a Dual Agilent Jet Stream technology source (product number G6575A) was also used.

Software

Agilent **MassHunter Acquisition software** for LC/Q-TOF, version 12.0, was used to operate the Revident LC/Q-TOF system.

Agilent **MassHunter Explorer software**, version 1.0, was used for feature extraction and differential analysis. For metabolite analysis, the Default-Metabolomics.M method was used with the following modifications: Height Filter: 1,500; Ion Species: $-\text{H}$, $+\text{CH}_3\text{COO}$; Enable multi-pass exhaustive grouping; Mass Tolerance ± 10 ppm; Score (MFE) ≥ 70 in at least 75% of data files in at least one sample group; Enable RT Correction (with reference data file). For lipid analysis, the Default-Metabolomics.M method was used with the following modifications: Height Filter: 600; Ion Species: $+\text{H}$, $+\text{NH}_4$, $+\text{Na}$; Enable multi-pass exhaustive grouping; RT Tolerance ± 0.15 minutes; Mass Tolerance ± 10 ppm; Score (MFE) ≥ 70 in at least 75% of data files in at least one sample group. For background subtraction in both projects, a fold-change test was applied to all groups against the extraction blank (control) with a cutoff of two and one minimum pair. Other parameters are provided in the figures.

Agilent **Mass Profiler Professional (MPP) software**, version 15.1, was used for further differential analysis and results visualization. Files (.pfa) were imported from the MassHunter Explorer project as the data source. The positive-ion lipid dataset was created with the "Lipidomics" experiment type. A percentile shift normalization algorithm (75%) was used, and datasets were baselined to the median of all samples.

Agilent **MassHunter Lipid Annotator software**, version 1.0, with the default method parameters was used, except only $[M + H]^+$ and $[M + NH_4]^+$ precursors were considered for positive-ion mode analysis. The FAHFA lipid class was deselected.

Cell culture

THP-1 cells cultured in supplemented RPMI medium were maintained between 2 and 8×10^5 cells/mL. Cell cultures were treated with $4.98 \mu\text{M}$ SU1498, $1.36 \mu\text{M}$ AG-879, or DMSO vehicle at a final DMSO content of 1% (v/v) for 2 or 18 hours. For 18-hour treatments, cells were seeded at a density of 6×10^5 cells/mL to reach a target density of 7.5×10^5 cells/mL after 18 hours. For 2-hour treatments, cells were taken from the cell culture that had been used on the previous day to prepare the 18-hour culture treatments, to maintain the same cell split and media conditioning of both the 2- and 18-hour treated cells before starting the Seahorse XF assay.

NovoCyte cell counting for sample normalization

Cell counting was used for both Seahorse XF Pro analyzer and LC/MS sample normalization and was completed using a NovoCyte Quanteon flow cytometer with NovoSampler Q and a procedure similar to one previously described.⁴ A $400 \mu\text{L}$ aliquot from the DMSO control sample was split into two $200 \mu\text{L}$ portions to create a live/dead cell sample control. One $200 \mu\text{L}$ aliquot was stored at room temperature while the second $200 \mu\text{L}$ aliquot was heated to 65°C for 10 minutes to create the dead cell control. After allowing the heated sample to cool at room temperature for several minutes, the live and dead cell samples were recombined and gently mixed. Two $100 \mu\text{L}$ aliquots from the live/dead sample and one $100 \mu\text{L}$ aliquot from each experimental sample were transferred to a U-bottom, 96-well plate. For cell viability analysis, a $1 \mu\text{L}$ aliquot of 7-AAD (0.1 mg/mL) was added to each sample except for one live/dead sample that was reserved as an unstained control. Samples were mixed gently by pipette and the plate was placed in the NovoSampler Q for data acquisition. The live/dead cell samples were used to define the live and dead cell gates during data analysis. For Seahorse XF Pro analyzer cell count normalization, the live cell count was used because only live cells contribute to the OCR and ECAR signals. For LC/MS cell count normalization, the total cell count was used, since all cells contribute to the peak abundance signals.

Seahorse XF Pro analyzer cell preparation

For 18-hour treatments, cell culture aliquots of 1.4 mL were added to 12-well plates; treatment compounds or vehicle were added, and the samples were mixed thoroughly. After 18 hours, samples were mixed well via pipette to create a homogenous cell suspension, then $100 \mu\text{L}$ aliquots were taken for cell counting. In parallel, 1 mL of each sample was transferred to a 1.5 mL microfuge tube and centrifuged for 5 minutes at $250 \times g$ at room temperature to pellet the cells. After the cell counts were completed, the supernatant was removed from the 1 mL cell culture aliquots. Then, Agilent Seahorse XF RPMI medium, including the treatment compounds or vehicle, was added to each sample at a volume that would provide 1 million cells/mL. A $50 \mu\text{L}$ aliquot of each sample was transferred to a Seahorse XFe96/XF Pro PDL cell culture microplate to seed 50,000 cells/well. After a 20-minute settling period in a non- CO_2 incubator, the cell culture microplate was centrifuged for 5 minutes at $300 \times g$ at room temperature. A further $130 \mu\text{L}$ Seahorse media with the appropriate treatment or vehicle was added to each well after cell seeding and before starting the Seahorse assay. For the 2-hour treatment, a single cell count was completed before resuspending the cells in Seahorse XF media; aliquoting the cells; adding the treatment compounds or vehicle; and transferring $50 \mu\text{L}$ aliquots from each treatment group to the PDL cell culture microplate. The cell settling period, centrifugation, and additional Seahorse media addition replicated the 18-hour treatment method.

Cell lysis and quenching for LC/MS metabolomics and lipidomics analysis

To prepare samples for LC/MS analyses, a previously described³ cellular extraction method that leverages TFE to lyse mammalian cells and quench metabolism under room temperature conditions was applied. Notably, TFE quenching overcomes the challenges of cold liquid quenching, improves safety, and is amenable to robotic automation. NovoCyte cell counts were used to calculate the cell culture volumes needed to harvest 1 million THP-1 cells per sample. The harvested cell samples were washed with 1 mL room-temperature PBS, then lysed and quenched at room temperature with $100 \mu\text{L}$ 1:1 trifluoroethanol:water, mixed with a vortex mixer, and allowed to incubate for 10 minutes at room temperature.

Bravo automated dual metabolite and lipid fractionation

Using a previously described³ automated method on the Bravo Metabolomics Sample Prep Platform (Figure 2), polar metabolites and lipids were sequentially extracted from the TFE cell lysates corresponding to vehicle- and drug-treated THP-1 cells. This method leveraged 96-well Agilent Captiva EMR–Lipid plates, which contain a unique solid sorbent that selectively retains lipids containing acyl hydrocarbon chains. Briefly, after the protein was precipitated, TFE-quenched extracts were added to the plate and proteins were caught on a filter above the Captiva EMR–Lipid sorbent. The polar metabolites flowed through the sorbent and the lipids were captured on the sorbent. The polar metabolites in the flow

through were dried and then reconstituted in 200 µL 4:1 acetonitrile:water prior to HILIC-LC/MS analysis. A different collection plate was used for lipid elution, where the lipids were eluted with a stronger elution solvent and were then dried and reconstituted with 200 µL 9:1 methanol:chloroform for reversed-phase (RP) LC/MS analysis. To assist with reconstitution, both plates were shaken at 500 rpm for 20 minutes at room temperature. For Iterative MS/MS experiments, a five-times concentrated, pooled lipid sample was prepared by combining 20 µL aliquots from all wells with treatment replicates, drying under vacuum, and resuspending in one-fifth volume with 9:1 methanol:chloroform in a separate vial.

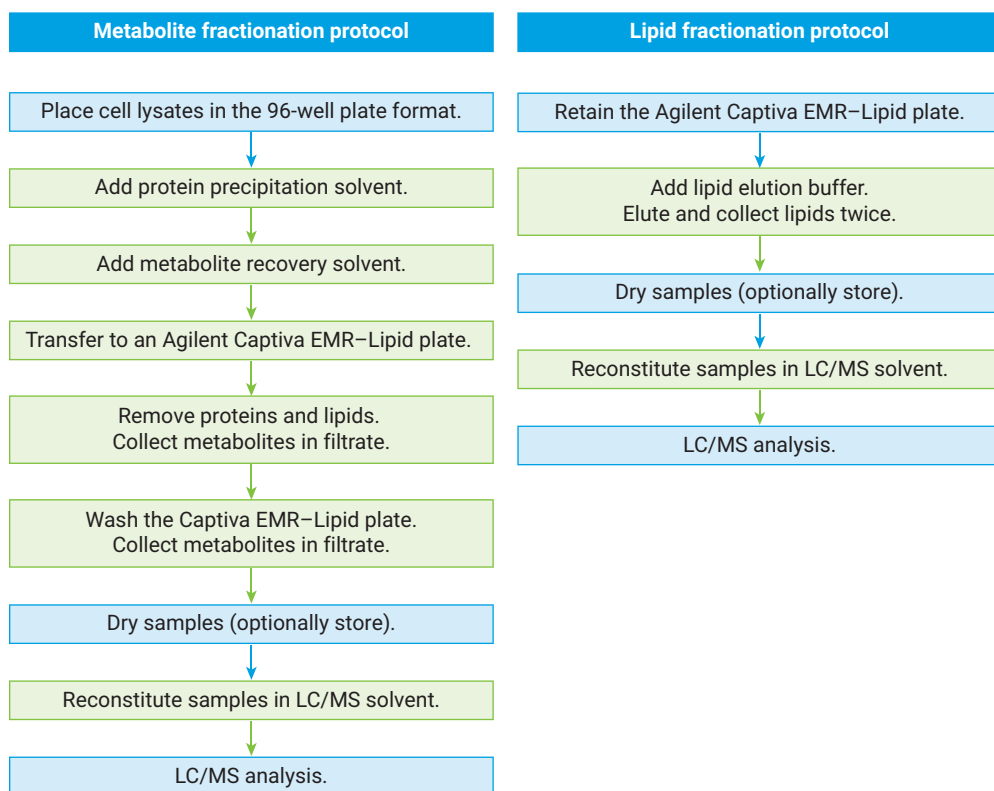


Figure 2. Method for automated dual metabolite + lipid fractionation of cell lysates.³ Green steps are performed with the Agilent Bravo Metabolomics Sample Prep Platform.

LC/MS methods

Metabolite HILIC LC method parameters were adapted from a previous application note.⁵ Lipid LC method parameters were adapted from a previous application note.⁶ Detailed experimental methods for LC conditions and LC/Q-TOF auto MS/MS parameters are provided in Tables 1 to 4. Additionally, negative-ion metabolite LC/Q-TOF MS-only data were acquired on the individual samples, with an MS acquisition rate of two spectra/second. Positive-ion lipid LC/Q-TOF All Ions data were acquired on the individual samples, with an acquisition rate of 8 spectra/second and collision energies of 0, 10, 20, and 40 eV. All worklists were randomized.

Table 1. Metabolite HILIC-LC instrument parameters.

Parameter	Agilent 1290 Infinity II Bio LC		
Analytical Column	Agilent InfinityLab Poroshell 120 HILIC-Z, 2.1 × 150 mm, 2.7 μm (p/n 683775-924)		
Inline Filter	Agilent 1290 Infinity II Bio inline filter kit, 0.3 μm (p/n 5720-0020)		
Column Temperature	15 °C		
Injection Volume	10 μL (MS and MS/MS)		
Autosampler Temperature	5 °C		
Needle Wash	Standard wash, 10 s, isopropanol:ACN:water 1:1:1		
Mobile Phase	A: 20 mM Ammonium acetate and 5 μM Agilent InfinityLab deactivator additive (p/n 5191-3940) in water, pH 9.3 B: ACN		
Gradient Program	Time (min)	%B	Flow Rate (mL/min)
	0	90	0.4
	1	90	0.4
	8	78	0.4
	12	60	0.4
	15	10	0.4
	18	10	0.4
	19	90	0.4
	19.1	90	0.5
	22	90	0.5
	22.1	90	0.4
	23	90	0.4
Stop Time	23 min		
Post-Time	None		

Table 2. Metabolite LC/Q-TOF instrument parameters.

Auto MS/MS Method Parameter	Agilent Revident LC/Q-TOF
Instrument Mode	750 Fragile
Ion Source	Agilent Dual Jet Stream
Polarity	Negative
Gas Temperature	225 °C
Drying Gas (Nitrogen)	9 L/min
Nebulizer Gas	40 psi
Sheath Gas Temperature	375 °C
Sheath Gas Flow	12 L/min
Capillary Voltage	3,000 V
Nozzle Voltage	500 V
Fragmentor	100 V
Skimmer	45 V
OctopoleRF Vpp	750 V
Reference Mass	m/z 112.985587, m/z 980.016375
MS Range	m/z 50 to 1,400
MS/MS Range	m/z 25 to 1,000
MS Acquisition Rate	8 spectra/s
Minimum MS/MS Acquisition Rate	6 spectra/s
Isolation Width	Narrow (~ 1.3 m/z)
Collision Energy	10, 20, and 40 eV
Maximum Precursors per Cycle	2
Variable Acquisition Rate	Yes, target count MS/MS: 25,000
Use MS/MS Accumulation Time Limit	Yes
Reject Precursors That Cannot Reach Target TIC	No
Precursor Threshold	5,000 counts and 0.001%
Active Exclusion	Disabled
Purity	Stringency 100%, cutoff 30%
Isotope Model	Common organic molecules
Precursor Charge-State Selection and Preference	1, 2, Unknown, by charge state
m/z Inclusion Range	m/z 50 to 1,400
Iterative MS/MS Mass Error Tolerance	20 ppm
Iterative MS/MS RT Exclusion Tolerance	± 0.2 min

Table 3. Lipid RP-LC Instrument parameters.

Parameter	Agilent 1290 Infinity II Bio LC																						
Analytical Column	Agilent ZORBAX Eclipse Plus C18, 100 x 2.1 mm, 1.8 µm (p/n 959758-902)																						
Inline Filter	Agilent 1290 Infinity II Bio inline filter kit, 0.3 µm (p/n 5720-0020)																						
Column Temperature	45 °C																						
Injection Volume	5 µL (All Ions and auto MS/MS)																						
Autosampler Temperature	20 °C																						
Needle Wash	Standard wash, 10 s, 1:1 mobile phase A:B																						
Mobile Phase	A: 10 mM ammonium formate, 0.2 mM ammonium fluoride, and 5 µM InfinityLab deactivator additive in 5:3:2 water:acetonitrile:isopropanol B: 10 mM ammonium formate and 0.2 mM ammonium fluoride in 1:9:90 water:acetonitrile:isopropanol																						
Flow Rate	0.4 mL/min																						
Gradient Program	<table> <tr> <th>Time (min)</th><th>%B</th></tr> <tr><td>0</td><td>15</td></tr> <tr><td>2.5</td><td>50</td></tr> <tr><td>2.6</td><td>57</td></tr> <tr><td>9</td><td>70</td></tr> <tr><td>9.1</td><td>93</td></tr> <tr><td>11</td><td>96</td></tr> <tr><td>11.1</td><td>100</td></tr> <tr><td>12</td><td>100</td></tr> <tr><td>12.2</td><td>15</td></tr> <tr><td>16</td><td>15</td></tr> </table>	Time (min)	%B	0	15	2.5	50	2.6	57	9	70	9.1	93	11	96	11.1	100	12	100	12.2	15	16	15
Time (min)	%B																						
0	15																						
2.5	50																						
2.6	57																						
9	70																						
9.1	93																						
11	96																						
11.1	100																						
12	100																						
12.2	15																						
16	15																						
Stop Time	16 min																						
Post-Time	None																						

Table 4. Lipid LC/Q-TOF Instrument parameters.

Auto MS/MS Method Parameter	Agilent Revident LC/Q-TOF
Instrument Mode	1,700 Stable
Ion Source	Agilent Dual Jet Stream
Polarity	Positive
Gas Temperature	320 °C
Drying Gas (Nitrogen)	8 L/min
Nebulizer Gas	45 psi
Sheath Gas Temperature	350 °C
Sheath Gas Flow	11 L/min
Capillary Voltage	3,500 V
Nozzle Voltage	1,000 V
Fragmentor	175 V
Skimmer	45 V
OctopoleRF Vpp	750 V
Reference Mass	<i>m/z</i> 121.050873, <i>m/z</i> 922.009798
MS Range	<i>m/z</i> 100 to 1,700
MS/MS Range	<i>m/z</i> 50 to 1,700
MS Acquisition Rate	3 spectra/s
Minimum MS/MS Acquisition Rate	3 spectra/s
Isolation Width	Narrow (~ 1.3 <i>m/z</i>)
Collision Energy	20 eV
Maximum Precursors per Cycle	3
Variable Acquisition Rate	Yes, target count MS/MS: 25,000
Use MS/MS Accumulation Time Limit	Yes
Reject Precursors That Cannot Reach Target TIC	No
Precursor Threshold	5,000 counts and 0.001%
Active Exclusion	Enabled, exclude after 2 spectra, release after 0.05 minutes
Purity	Stringency 70%, cutoff 0%
Isotope Model	Common organic molecules
Precursor Charge-State Selection and Preference	1, 2, Unknown, by abundance
<i>m/z</i> Inclusion Range	<i>m/z</i> 151 to 1,700
Iterative MS/MS Mass Error Tolerance	20 ppm
Iterative MS/MS RT Exclusion Tolerance	± 0.1 min

Results and discussion

Seahorse XF Pro analyzer reveals drug treatment perturbs glycoATP and mitoATP production rates through mitochondrial uncoupling

In a previous application note¹, a tyrosine kinase inhibitor library of 80 compounds was screened with the Seahorse XF Real-Time ATP rate assay to assess acute effects of the inhibitors on mitochondrial (mitoATP) and glycolytic (glycoATP) ATP production rates in both cancerous THP-1 and healthy peripheral blood mononuclear cells (PBMCs). From these results, two compounds were selected for further study in this application note based on their activity: AG-879 reduced mitoATP production rates in both THP-1 cancer cells and healthy PBMCs, while SU1498 reduced mitoATP production rates in cancerous THP-1 cells, but not in healthy PBMCs. Here, additional Seahorse XF characterization on the metabolic effects of these compounds was performed.

As a first step, the Seahorse XF Real-Time ATP rate assay was used to measure both acute (2 hours) and longer-term (18 hours) treatment impacts of the two selected drugs on mitoATP and glycoATP production rates. Drug treatment concentrations used the previously determined mitoATP half-maximal inhibitory concentrations (IC_{50}).¹ For both treatment lengths, AG-879 and SU1498 caused an increased glycoATP production rate to compensate for a reduced mitoATP production rate (Figures 3A and B). After the 18-hour treatment, total ATP production rates were reduced by 20 to 30% as compared to the 18-hour DMSO vehicle control, indicating that acute effects of AG-879 and SU1498 were amplified with longer treatment. Since cells were plated for the Seahorse assay based on live, viable cell counts, the decrease in total ATP production with kinase inhibitor treatment was not due to loss of cell viability. Notably, cell viability remained high (> 92%) after 18-hour treatments and was consistent across vehicle control and drug treatment groups (Figure 3C).

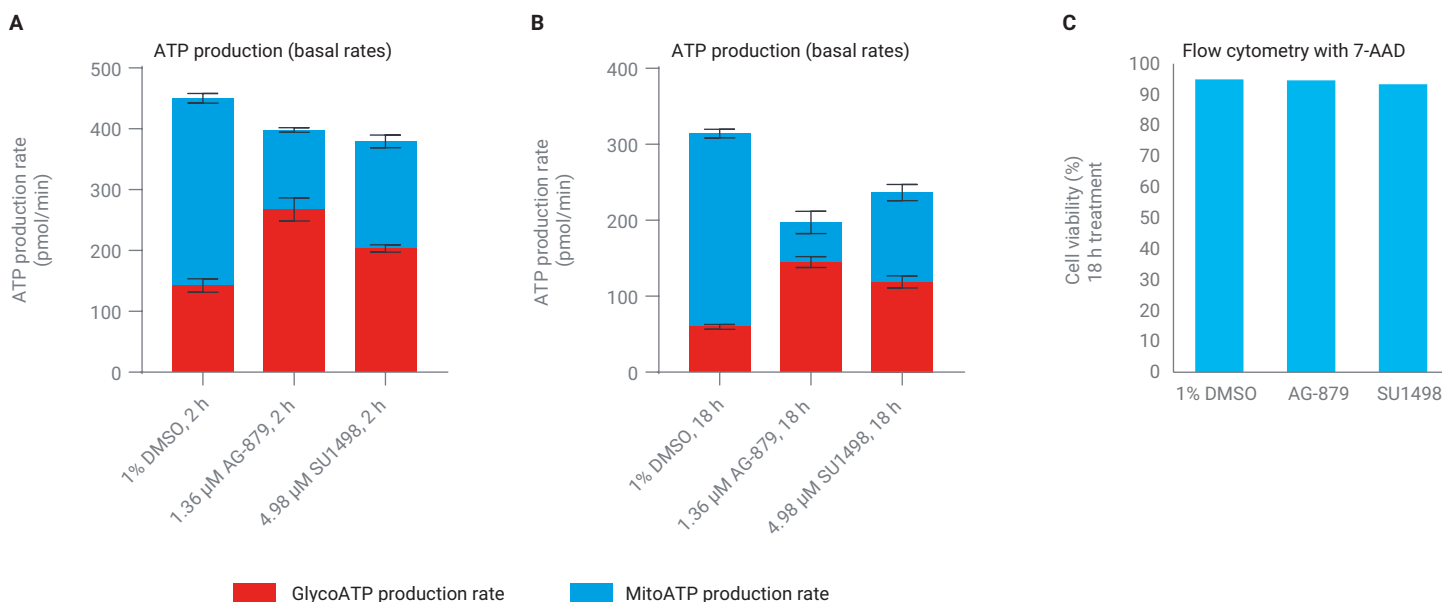


Figure 3. Agilent Seahorse XF Real-Time ATP rate assay demonstrates modulation of mitochondrial and glycolytic ATP production rates with drug treatment. THP-1 cells were pretreated with the vehicle control (1% DMSO), 1.36 μ M AG-879, or 4.98 μ M SU1498 for (A) 2 hours and (B) 18 hours, and analyzed for mitoATP and glycoATP production rates. (C) Cell viability was measured after 18-hour treatments by flow cytometry and staining with 7-AAD.

For a deeper investigation of drug impact on mitochondrial respiration rates, proton leak and SRC were analyzed, which are typical measurements provided by the Seahorse XF Mito Stress Test kit. Proton leak was used to quantify the degree of mitochondrial uncoupling in cells from the various treatment groups. Mitochondrial uncoupling is a term indicating that the cells still consume oxygen through the mitochondrial transport chain but are no longer able to efficiently generate ATP from this oxygen consumption, hence protons are leaked. Both tyrosine kinase inhibitors were demonstrated to be "mitochondrial uncouplers" due to the increased proton leak compared to vehicle-treated cells (Figure 4A). To compensate for the mitochondrial uncoupling, the cells increase their glycoATP rate (Figures 3A and B).

AG-879 and SU1498 caused THP-1 mitochondrial uncoupling with differing kinetics. Specifically, the AG-879-induced proton leak increased from 2 to 18 hours of treatment, suggesting a relatively slow uncoupling effect (Figure 4A). In contrast, the SU1498-induced proton leak decreased between 2 and 18 hours of treatment, suggesting a faster onset of uncoupling and that the cells were beginning to downregulate oxygen consumption at 18 hours in response to uncoupling that occurred earlier. This downregulation of oxygen consumption could cause perturbations in the relative levels of tricarboxylic acid (TCA) cycle intermediates, which were assessed by LC/MS metabolomics analysis. Moreover, it was found that SU1498 reduced SRC—a property often associated with cell fitness (Figure 4B). AG-879 caused a complete loss of SRC, suggesting cells treated with AG-879 likely have a lower capacity to employ survival signaling that may drive drug resistance through metabolic reprogramming.

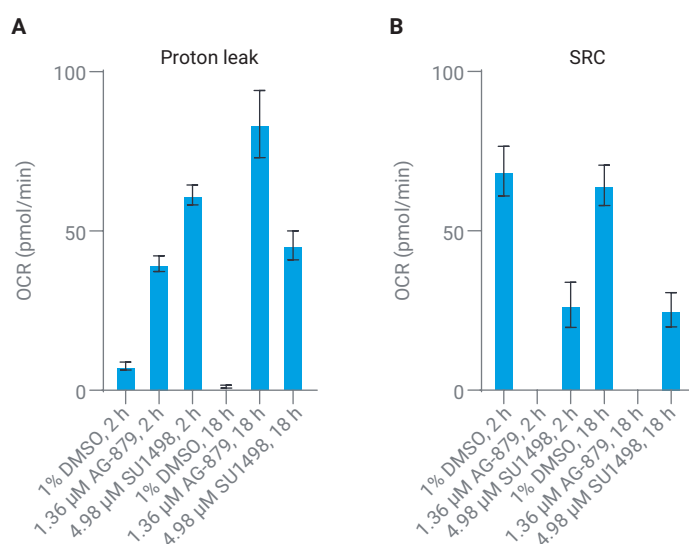


Figure 4. AG-879 and SU1498 treatment caused mitochondrial uncoupling and reduced cell fitness. THP-1 cells were pretreated with the vehicle control (1% DMSO), 1.36 μ M AG-879, or 4.98 μ M SU1498 for 2 and 18 hours, and were analyzed for (A) proton leak and (B) SRC.

Untargeted metabolomics identified changes in key metabolites associated with glycolysis and mitochondrial respiration that correlate with Seahorse XF Pro analyzer results

The reconstituted 96-well metabolite fraction plate was placed in a 1290 Infinity II Bio LC, which consists of a special biocompatible alloy, MP35N. This iron-free flow path demonstrates superior performance for the analysis of phosphorylated compounds.⁶ Extracts were separated with a previously established, robust HILIC chromatography method that is well suited for separation of cellular metabolites.⁵ LC eluents were analyzed with a Revident LC/Q-TOF, which delivers improved spectral quality resulting in increased mass resolution, dynamic range, and isotopic fidelity.

The HILIC LC/Q-TOF dataset was processed with MassHunter Explorer—software that provides a workflow-guided user interface and combines data extraction, normalization, data analysis, and identification of features for nontargeted LC/Q-TOF data into a single application. To enable differential analysis and find metabolites affected by drug treatment, the vehicle control, AG-879, SU1498, and extraction blank data files were added to a MassHunter Explorer project.

Following data extraction and normalization, compounds that were detected at similar levels in both the extraction blanks and cell samples were removed from the project, leaving 1,802 compound groups. Next, several compound groups with mass values corresponding to the SU1498 and AG-879 drugs were removed from the project, leaving 1,797 compound groups. The MassHunter Explorer graphical user interface (GUI) allows the user to move forward and backward in the navigation ribbon, and the results from the different workflow procedures are linked. In this case, compound groups were identified first before moving to statistics. To identify endogenous metabolites, a database search was performed against a 471-compound subset of the Agilent METLIN Personal Compound Database and Library curated with HILIC-Z retention times from authentic chemical standards.⁵ Both mass and retention time were selected as required database (DB) matching criteria, resulting in 101 out of 1,797 annotated compound groups (Figure 5). Considering that the DB search was performed with ± 5 ppm mass error tolerance, 79 of 101 compounds showed an observed Δ ppm of < 1.0 , demonstrating the excellent mass accuracy of the Revident LC/Q-TOF.

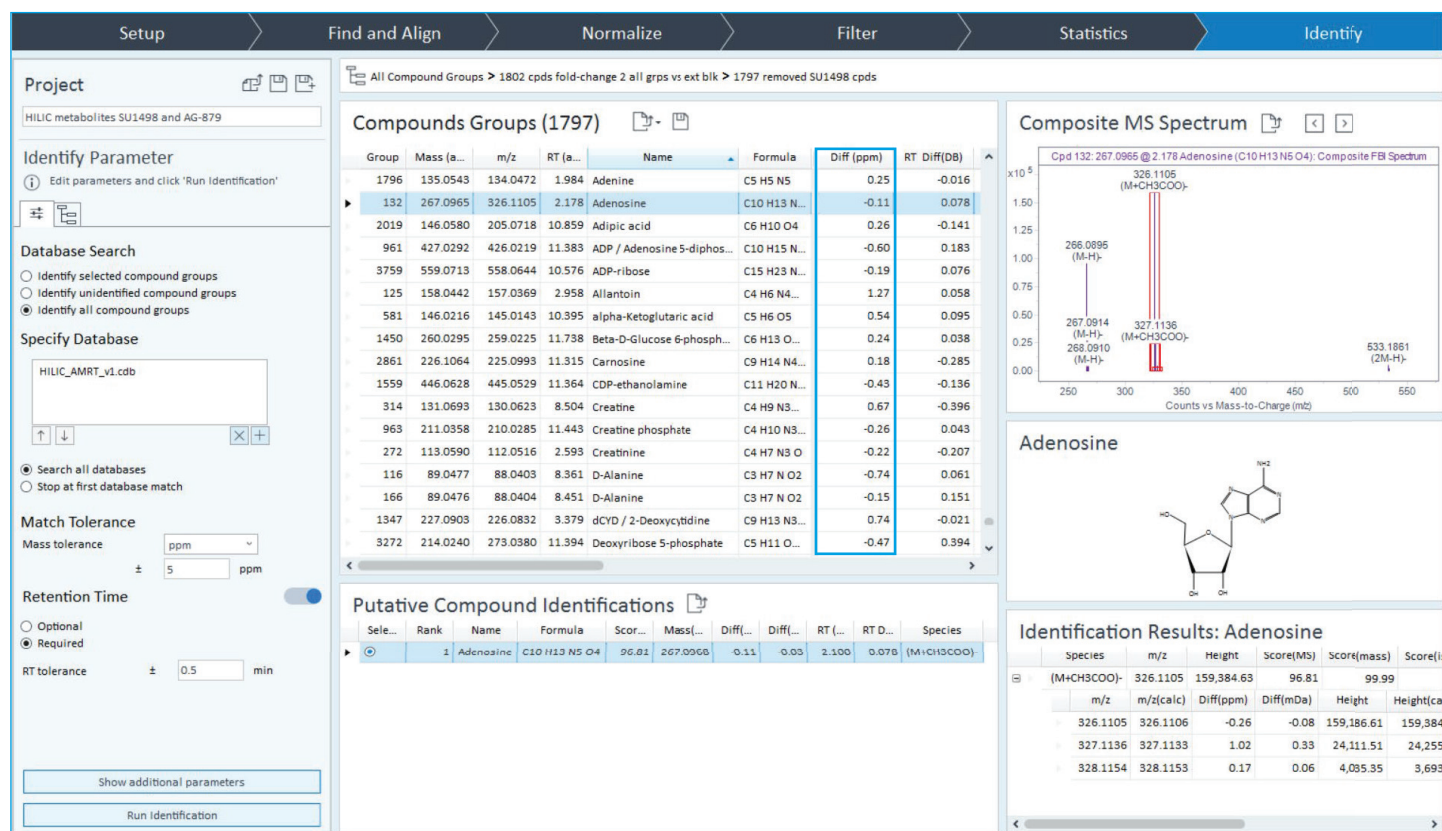


Figure 5. Agilent MassHunter Explorer software GUI displaying results from the "Identify" procedure. A curated DB containing 471 compounds with HILIC RTs was specified, resulting in 101 annotated compound groups—a portion of which are shown. The mass tolerance was ± 5 ppm and the RT tolerance was ± 0.5 minutes. The observed Δ ppm values are highlighted in the blue box.

Volcano plots were used as the statistical test to identify compound groups that exhibited substantial differences between the drug-treated sample groups and the vehicle control group. For the SU1498-treated samples,

131 compound groups displayed statistical significance with a fold-change > 1.5 and $P < 0.05$ (Figure 6). With the same statistical test, only six compound groups displayed significance in the AG-879 volcano plot (not shown).

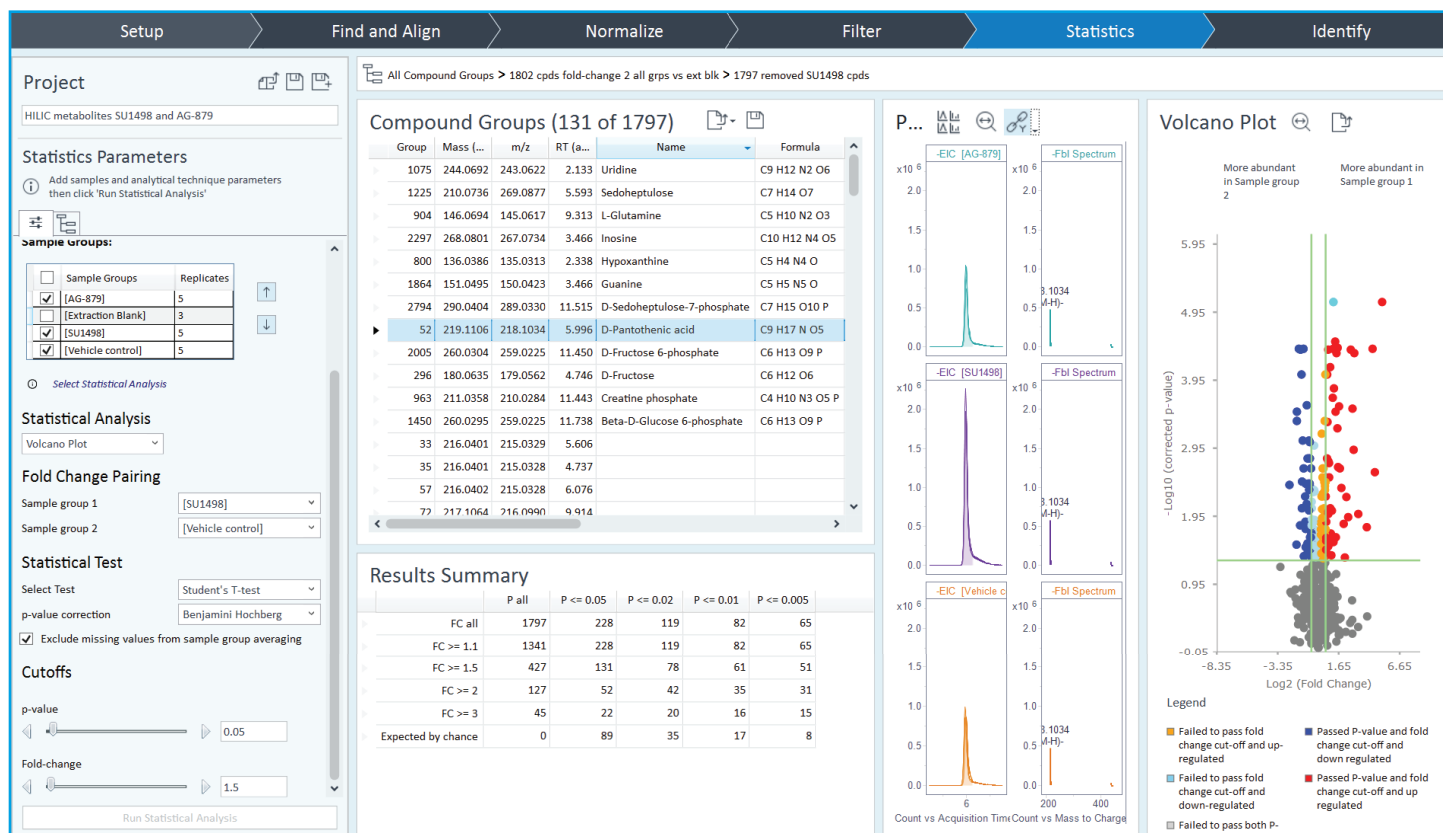


Figure 6. Agilent MassHunter Explorer software GUI displaying results from the "Statistics" procedure. A volcano plot was performed on the SU1498 treatment group paired against the vehicle control group, with the applied parameters shown. The annotated compound group for d-pantothenic acid is selected. Corresponding extracted ion chromatograms and mass spectra are linked for immediate visualization and verification, and the corresponding data point in the volcano plot is automatically highlighted in light blue.

The MassHunter Explorer software GUI displays a Principal Component Analysis (PCA) plot that automatically updates with every applied normalization step, filter, and statistical test. A PCA based on the 131 significant compound groups showed clear separation between drug-treated and vehicle control groups (Figure 7A). The principal component 1 (X-axis) contributed the most to the variability (68%) of the plot, and the AG-879 group was between SU1498 and vehicle control groups. Figure 7B illustrates the comparison of AG-879 and SU1498 results and behavior of the annotated metabolites. Notably, all six significant compound groups from AG-879 treatment were also observed with SU1498 treatment, and the three shared annotated metabolites were decreased with both drug treatments. Taken together, the (1) degree of separation of sample groups by PCA, (2) lower number of significant compound groups in AG-879, and (3) shared behavior of metabolites in both treatments all suggest that AG-879 treatment induced similar but muted effects on cellular metabolism compared to SU1498 treatment. Since the mitochondrial uncoupling kinetics appeared to be slower in response to AG-879 as compared to SU1498, it is possible that a longer treatment with AG-879 may lead to detection of significant increases and decreases in more compound groups than was seen after 18 hours of AG-879 treatment. Alternatively, the more muted effects of AG-879 may be caused by the lack of SRC in these cells, which may reduce the capacity of the cells to use alternative metabolic pathways.

Several conclusions may be drawn from the observed increase/decrease of specific metabolites in relation to the Seahorse XF Pro analyzer results. For both drug treatments, there was a reduction in several sugar phosphates that belong to both glycolysis and the parallel pentose (PP) phosphate pathway. Seahorse XF Pro analyzer results showed increased glycoATP rates (Figure 3) for both drug treatments, and, together, this suggests that the increase in glycolysis (and likely the PP pathway) depletes glycolytic intermediates, including sugar phosphates. Conversely, there was an increase in pantothenic acid in the SU1498 treatment, which is a precursor for Coenzyme A (CoA) required for the TCA cycle and lipid biosynthesis. As a reminder, the proton leak data from SU1498 treatment suggested a downregulation of the TCA cycle after 18 hours of treatment, which would correlate well with an accumulation of this precursor compound. The most pronounced changes with SU1498 treatment were the marked increase in uridine, inosine, hypoxanthine, and guanine, which are all metabolites involved in purine and pyrimidine metabolism. The increased glycolytic and PP pathway flux may impact these metabolites, as ribose-5-phosphate is a precursor for purine and pyrimidine biosynthesis. Accordingly, L-glutamine, which is an additional precursor for purine/pyrimidine metabolism, was found to be reduced with SU1498 treatment. Thus, the LC/MS-based detection of perturbed metabolites outside of the primary energetic pathways identified with the Seahorse XF Pro analyzer illustrates an example where the insights gained from LC/MS may point to new vulnerabilities in these cells that could inform combinatorial treatment.

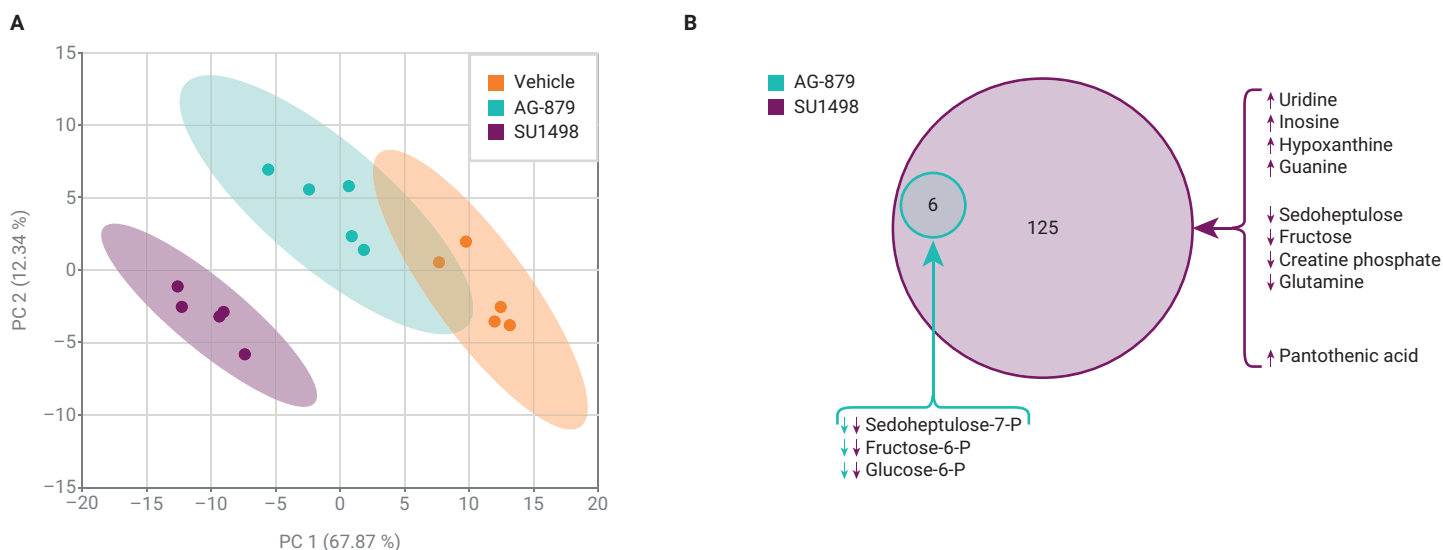


Figure 7. Comparison of AG-879 and SU1498 results. (A) PCA based on the 131 significant compounds. (B) Venn diagram showing the significant compound groups shared between AG-879 and SU1498 treatments, with annotated metabolites and direction of change indicated. Arrows indicate whether the metabolite levels were elevated (↑) or decreased (↓) in the drug treatment groups relative to the vehicle control group.

Untargeted lipidomics revealed changes in key lipids associated with glycolysis and mitochondrial respiration that correlate with Seahorse XF Pro analyzer and LC/MS metabolomics results

The reconstituted 96-well lipid plate was placed in the 1290 Infinity II Bio LC, connected to the Revident LC/Q-TOF, the same hardware configuration used for metabolite analysis. Instead of HILIC-LC, extracts were separated with an established RP-LC method optimized for lipid separation⁵, and eluents were analyzed on the Revident LC/Q-TOF in positive-ion mode.

Lipidomics data analysis followed a similar workflow to the metabolite analysis described previously. First, to enable differential analysis and find lipids affected by drug treatment, the vehicle control, AG-879, SU1498, and extraction blank data files were added to a MassHunter Explorer project. Following data extraction and normalization, compounds that were detected at similar levels in both the extraction blanks and cell samples were removed from the project, leaving 2,662 compound groups.

Compound groups were annotated before moving to statistics. To enable lipid annotation, MassHunter Lipid Annotator software was first used to build a lipid database. The lipid database was based on in silico MS/MS spectral

library matching from MS/MS spectra that were acquired from representative pooled cellular extracts combined from the THP-1 cells and treatments used in this study as well as from K562 cells and treatments used in a different study. Specifically, a set of six positive-ion and six negative-ion mode iterative MS/MS data files were analyzed. This resulted in 562 lipids—representing 16 classes—annotated for positive-ion mode (Figure 8A), and 500 lipids—representing 22 classes—annotated for negative-ion mode (Figure 8B). MassHunter Lipid Annotator software results were exported, and the resulting database (.cdb) files were searched sequentially in MassHunter Explorer software to map the annotations to compound groups in the MassHunter Explorer project (Figure 8C). While the MassHunter Explorer project was created from data files of positive ions only, the calculated neutral mass of compound groups enabled matching against the neutral mass from the databases regardless of polarity. A strategy of additionally searching the negative-ion database resulted in more annotations and a higher degree of specificity in some annotations, as acyl chain information can more often be deduced from negative-ion mode MS/MS data. Both mass and retention time were selected as required DB matching criteria, resulting in annotations for 507 of the 2,662 compound groups covering 23 lipid classes.

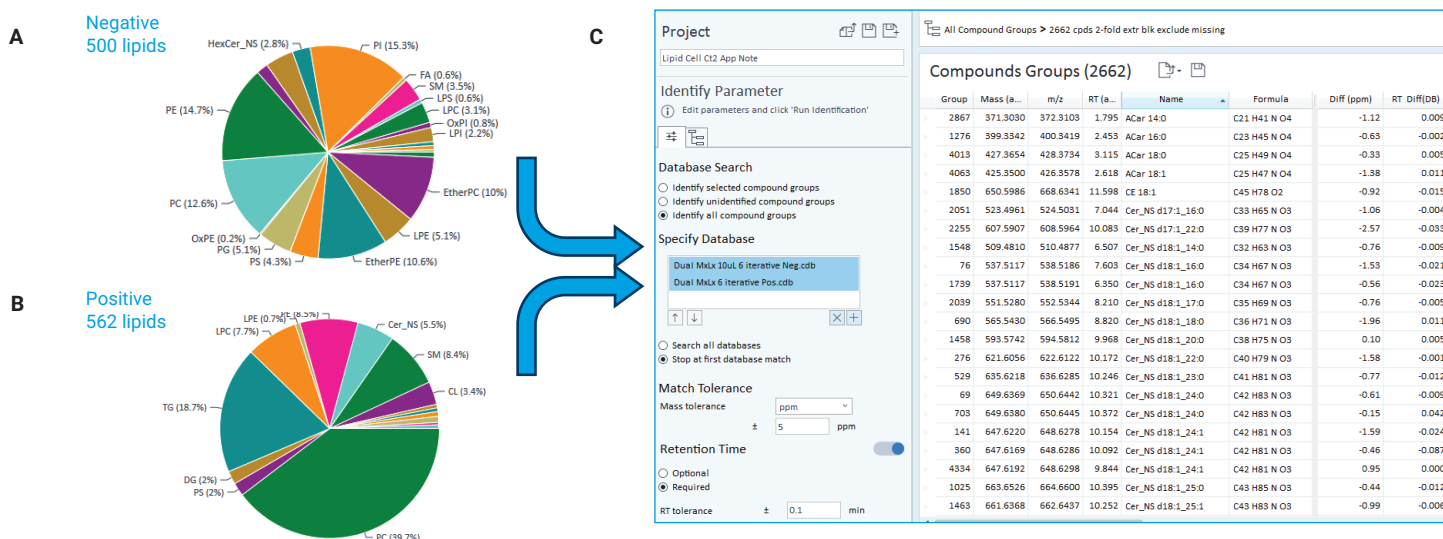


Figure 8. Lipid annotation strategy. Six iterative MS/MS data files were analyzed as a batch in Agilent MassHunter Lipid Annotator software. Shown are pie charts with the percentages of major lipid classes for (A) negative and (B) positive ionization modes. (C) The databases were leveraged sequentially in the Identify workflow step of Agilent MassHunter Explorer software. The mass tolerance was ± 5 ppm and the RT tolerance was ± 0.1 minutes.

Volcano plots were similarly used to pull out significant lipid compounds as was done with the metabolites. For the SU1498-treated samples, 521 compound groups displayed statistical significance with a fold change of > 1.5 and $P < 0.05$ (Figure 9A). With the same statistical test, only 23 compound groups displayed significance in the AG-879 volcano plot (Figure 9B). A PCA plot based on the 521 significant compounds showed a clear distinction between the drug-treated and vehicle control groups (Figure 9C), and the Venn diagram shows that all 23 of the significant compound groups from AG-879 treatment were also observed with SU1498 treatment (Figure 9D). Altogether, these lipid results closely mirrored the metabolite results, again suggesting that AG-879 treatment induces similar but muted effects on cellular metabolism compared to SU1498 treatment. Again, this may be a result of slower kinetics of the AG-879 treatment suggested by the proton leak data or the lack of SRC in AG-879 treated cells. Regarding annotated

lipids, the most pronounced result was the increase in 62 triglyceride (TG) lipids, showing an up to eight-fold increase in SU1498 relative to the vehicle control. The increase in TG content may, like pantothenic acid, be related to buildup of energy precursors following TCA cycle downregulation, as suggested by the SU1498 proton leak data identified using the Seahorse XF Pro analyzer. Alternatively, the combination of a decrease in glutamine levels and an increase in TGs suggests that SU1498-treated cells may be adapting to the treatment by reprogramming and implementing anaplerosis, where glutamine is used to fuel the TCA cycle for lipid production. This may also explain the increase in pantothenic acid, as the acetyl-CoA produced during anaplerosis is a feedback inhibitor of pantothenic acid kinase, which converts pantothenic acid into 4'-phosphopantothenic acid. In some cases, anaplerosis is used to support glyconeogenesis to fuel the increased glycolytic flux being used for glycoATP production and other biosynthetic processes.

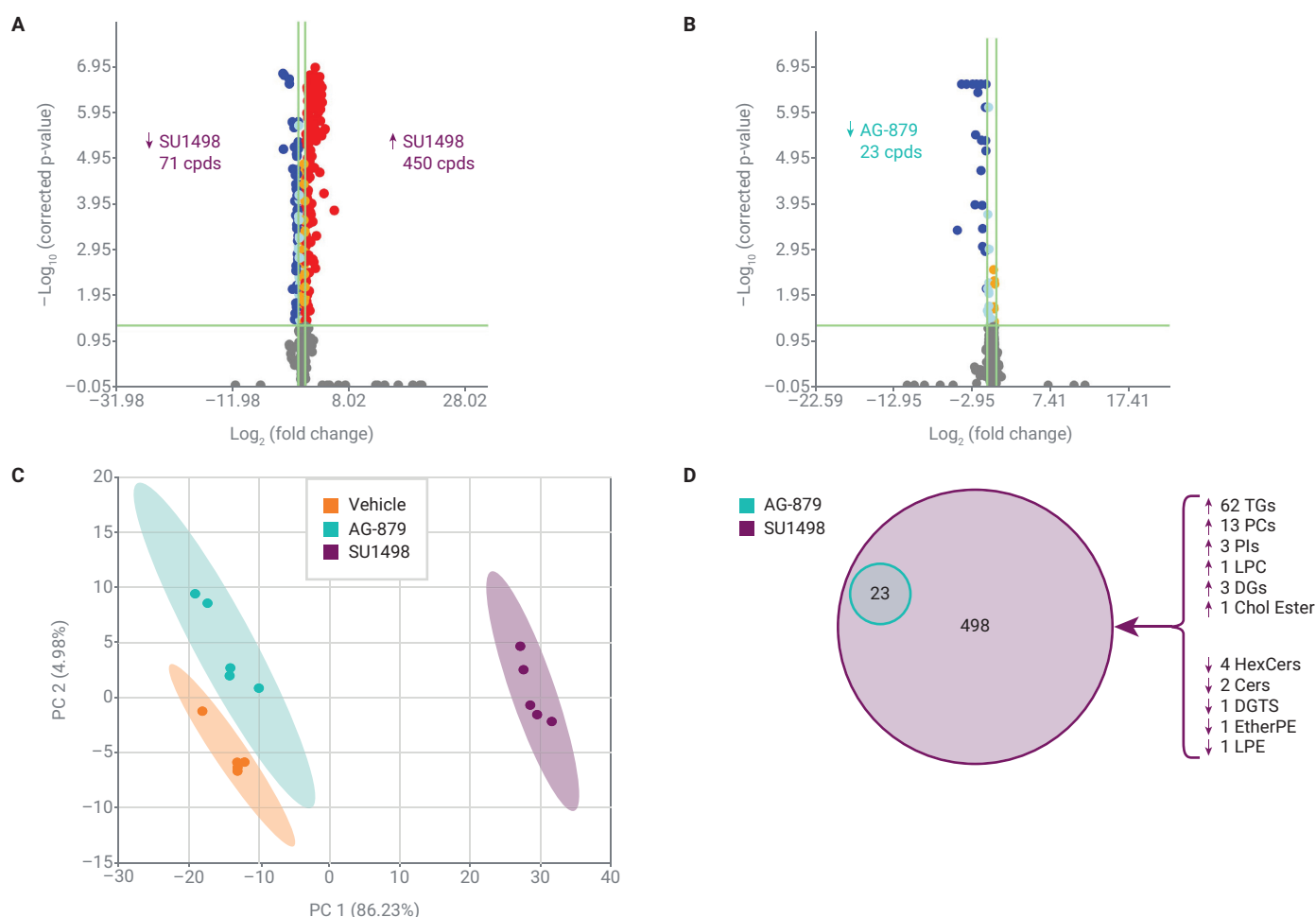


Figure 9. Comparison of AG-879 and SU1498 lipid results. Volcano plot analyses performed on (A) the SU1498 treatment group paired against the vehicle control group and (B) the AG-879 treatment versus vehicle. (Student's t-test, $FC > 1.5$, $P < 0.05$, with Benjamini-Hochberg correction.) (C) PCA based on the 521 significant compounds. (D) Venn diagram showing the significant compound groups shared between AG-879 and SU1498 treatments, with 92 annotated lipids and direction of change indicated. Arrows indicate whether the lipid levels were elevated (\uparrow) or decreased (\downarrow) in SU1498 treatment.

MassHunter Explorer software results can be exported to MPP to enable advanced statistics and visualizations. Therefore, for deeper insight into lipid results, the MassHunter Explorer project was exported as a .pfa file into MPP. Lipid matrix plots were created to enable visualization of abundance differences within lipid classes. The lipid class matrix plot based on TG clearly showed almost universally increased abundance for TG lipids in the SU1498 compared to the vehicle control (Figure 10A), which was similarly deduced from the MassHunter Explorer volcano plot described

previously. However, the matrix plot additionally revealed fine differences in TG lipid profiles, showing that TGs of higher double-bond content generally were more increased with SU1498 treatment. Inspection of the lipid class matrix plot based on phosphatidylinositols (PIs) revealed that the PI profile remained generally unchanged except for two specific lipid species—PI 18:1_18:2 and PI 38:6 (Figure 10B). MS/MS spectra of these lipids showed evidence for esterification with polyunsaturated acids (PUFAs), namely lineoleic acid (18:2) and arachidonic acid (20:4), both of which feed into

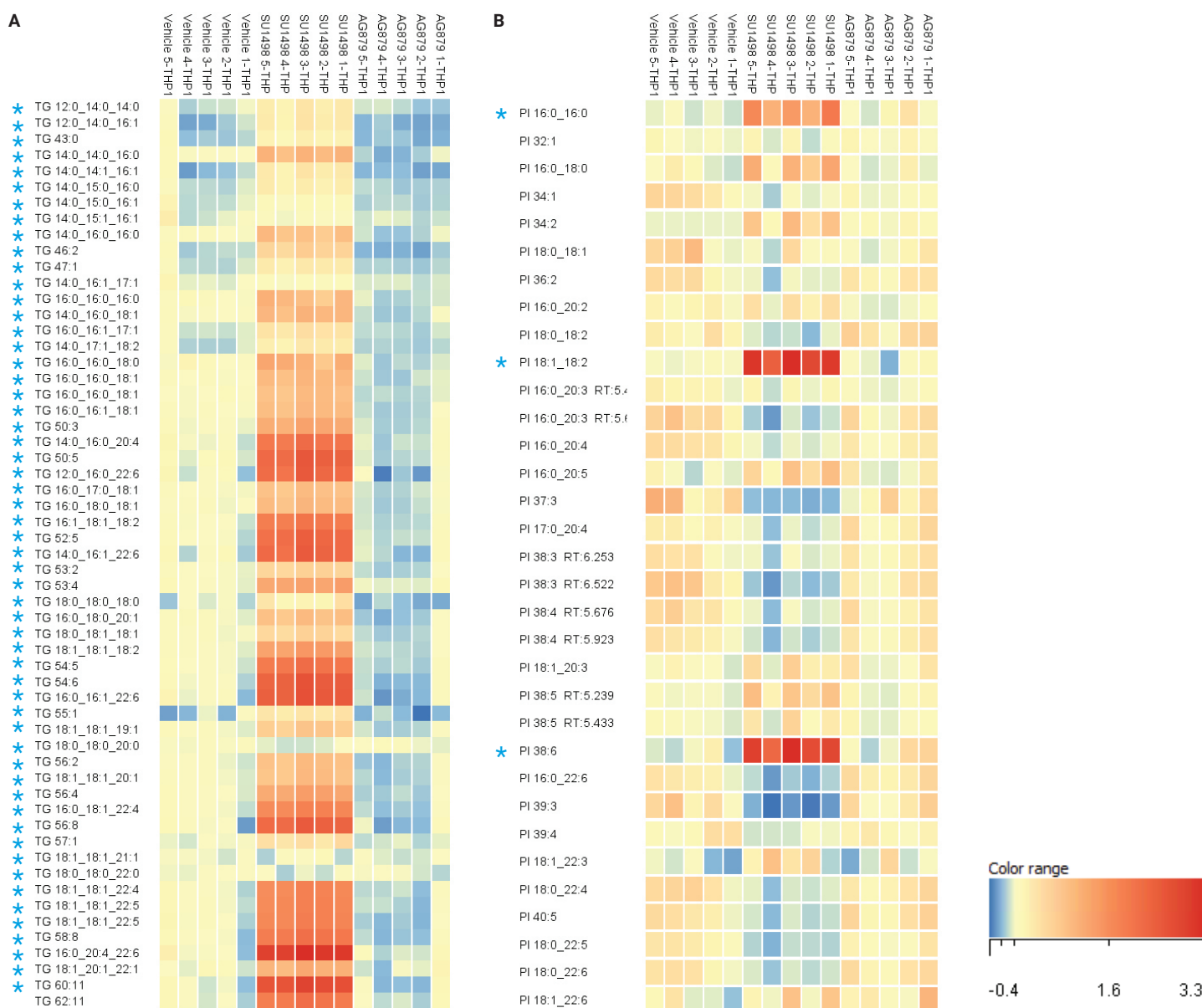


Figure 10. Agilent MPP software lipid matrix plots of (A) 57 TG and (B) 33 PI lipid features across SU1498 treatment, AG-879 treatment, and vehicle control sample replicates. Significant compounds that increased with SU1498 treatment, determined by Agilent MassHunter Explorer software volcano plot analysis, are indicated with a blue asterisk (*).

eicosanoid biosynthesis (not shown). It is known that PI serves as a reservoir for these signaling fatty acids and that these specific PI lipids are reduced in cancer cells, particularly cells with p53 mutations such as the THP-1 cell line used in this study. The results demonstrate that SU1498 treatment increases the level of these PI lipids in THP-1 cells, which may impact the downstream signaling biology of these cells.

Conclusion

This application note demonstrates an end-to-end workflow combining the Agilent Seahorse XF Pro analyzer and Q-TOF LC/MS that provided deeper insight into the cellular and molecular metabolic response of cancer cells to drug treatment. Specifically, XF analysis of AG-879 and SU1498 treatments corroborated previous results¹, and newly demonstrated that both drugs cause mitochondrial uncoupling. Untargeted metabolomics identified changes in key metabolites affected in glycolysis and mitochondrial respiration that correlate with XF results, and additionally identified affected metabolites involved in purine/pyrimidine metabolism. Untargeted lipidomics showed an increase in TG content with SU1498 treatment and enrichment in PUFA-containing PI lipids, the latter being potentially indicative of altered signaling biology with SU1498 treatment. Notably, the combination of results, including mitochondrial uncoupling (XF), decreased glutamine and increased pantothenic acid (metabolomics), and greatly increased TGs (lipidomics) led to consideration of a new hypothesis that SU1498-treated cells had reprogrammed their signaling pathways to use anaplerosis to build lipids. Formation of this hypothesis was only possible through a combination of cell analysis techniques. The more limited metabolite and lipid alterations detected following AG-879 treatment may be due to a variety of factors, including the lack of SRC caused by AG-879, differing kinetics between the two inhibitors, and the selected drug concentrations. Future avenues of investigation could include (1) further mining of the unidentified significant features, (2) qualitative flux analysis with Agilent MassHunter VistaFlux software⁸, (3) use of the Agilent Seahorse XF Substrate Oxidation Stress Test kit to assess fuel dependencies with drug treatment, and (4) completion of similar studies with healthy PBMC cells for comparison of metabolic pathway perturbations to the THP-1 cancer cells.

References

1. Vander Heiden, M. G.; *et al.* Understanding the Warburg Effect: The Metabolic Requirements of Cell Proliferation. *Science* **2009**, 324(5930), 1029–1033.
2. Kam, Y.; *et al.* Rapid Bioenergetic Functional screening of Anticancer Drug Candidates. *Agilent Technologies application note*, publication number 5994-5651EN, **2023**.
3. Van de Bittner, G. C.; *et al.* An Automated Dual Metabolite + Lipid Sample Preparation Workflow for Mammalian Cell Samples. *Agilent Technologies technical overview*, publication number 5994-5065EN, **2022**.
4. Wang, G.; *et al.* Using the Agilent NovoCyte Flow Cytometer for Immune Suspension Cell Normalization in Agilent Seahorse XF Assays. *Agilent Technologies application note*, publication number 5994-6245EN, **2023**.
5. Yannell, K.; *et al.* An End-to-End Targeted Metabolomics Workflow. *Agilent Technologies application note*, publication number 5994-5628EN, **2023**.
6. Huynh, K.; *et al.* A Comprehensive, Curated, High-Throughput Method for the Detailed Analysis of the Plasma Lipidome. *Agilent Technologies application note*, publication number 5994-3747EN, **2021**.
7. Feith, A.; *et al.* Improved Metabolomic Analysis Using an Iron-Free Flow Path. *Agilent Technologies application note*, publication number 5994-4622EN, **2022**.
8. Wattanavanitchakorn, S.; *et al.* ¹³C Glucose Qualitative Flux Analysis in HepG2 cells. *Agilent Technologies application note*, publication number 5994-0713EN, **2019**.

www.agilent.com

RA45477.0354166667

For Research Use Only. Not for use in diagnostic procedures.

This information is subject to change without notice.

© Agilent Technologies, Inc. 2024
Printed in the USA, July 30, 2024
5994-7449EN